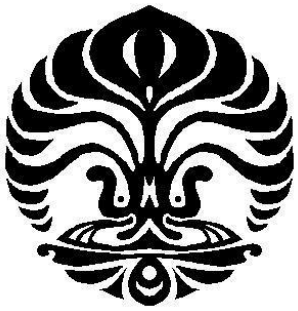

UNIVERSITY OF INDONESIA

EFFECT OF COOLING RATE AND TERNARY ADDITIONS OF CHROMIUM ON THE MICROSTRUCTURE OF Ti-Si EUTECTIC ALLOY

FINAL PROJECT

RAHARDIAN GHAZALI

0404840026

S-1 INTERNATIONAL PROGRAM

FACULTY OF ENGINEERING

DEPARTMENT OF METALLURGY AND MATERIALS ENGINEERING

DEPOK

JULY 2009

AUTHENTICATION PAGE

I state that this project proposal with the title below:

EFFECT OF COOLING RATE AND TERNARY ADDITIONS OF CHROMIUM ON THE MICROSTRUCTURE OF TI-SI EUTECTIC ALLOY

As far as I concern is not duplication from other project proposal which are published or has been used to obtain a degree in University of Indonesia, except some part which are referenced.

Name : Rahardian Ghazali

NPM : 0404840026

Signature :

Date : 17th July 2009

VALIDATION PAGE

This Final Project Report is proposed by:

Name : Rahardian Ghazali

NPM : 0404840026

Course Program : Metallurgy and Materials Engineering

Project Title : Effect of Cooling Rate and Ternary Additions of Chromium on the Microstructure of Ti-Si Eutectic Alloy

Produce in order to fulfill the requirement to become Sarjana Teknik in the Department of Material Engineering, Faculty of Engineering, University of Indonesia. This project report has been examined and approved on the project presentation.

Depok, July 2009

Supervisor,

Dr. Ir. Bondan Tiara Sofyan, M.si

NIP. 131 992 220

PREFACE

The research with the title "THE EFFECT OF COOLING RATE AND TERNARY ADDITIONS OF CHROMIUM ON THE MICRTOSTRUCTURE OF TI-SI EUTECTIC ALLOY" is accomplished as an academic requirement to obtain Bachelor of Engineering in Monash University and Sarjana Teknik in University of Indonesia.

The writer is aware that this research is still far from excellence and has many limitations, so it might be needed further improvement and deeper investigations.

The writer would like to express his gratitude to all those who gave him the possibility to complete this final year project report. Many thanks to:

- Allah SWT, for giving the strength, wisdom and conviction to finish this research
- My supervisor in Monash University, Dr. Colleen Bettles whose help, stimulating suggestions and encouragement helped me in all the time of research for and writing of this Final Report.
- My supervisor in University of Indonesia, Dr. Ir. Bondan Tiara Sofyan, M.Si for all her guidance, advice, patience and especially her support in this 5 years of my study both in University of Indonesia and Monash University.
- Dr. M. A. Gibson from CSIRO for his help in the preparation of the wedge casting
- Research Fellows and Staffs in Monash University, Dr. Hoi Pang Ng, Dr. Dacian Tomus, Mr. Daniel Curtis, Mr. Silvio Mattievich, and Mr. Ireneusz kozicki for providing me all laboratories tools, assisting in using the apparatus, and also time to share thoughts and ideas for this final year project.
- My beloved family, for always praying and giving both financial and spiritual support to accomplished this degree.
- All lecturers in both Monash University and University of Indonesia for all their guidance in this past 5 years of my study.
- My lovely friends in International Class, Faculty of Engineering, University of Indonesia; Haryman Lamhot Manulang, Diko Yudazaki, Dhiani Satiti, Rachmat

Imansyah, Leo Gading Mas, and Andhika Ibrahim for all their help, support, interest, and valuable hints

- All IMPI (Ikatan Mahasiswa Program Internasional) colleagues that cannot be mentioned one by one, for all wonderful experience.
- All staff in University of Indonesia
- And other indirect parties who had involved and gave their support in accomplishing this Final Year Project Report.

Depok, July 2009

Rahardian Ghazali

HALAMAN PERNYATAAN PERSETUJUAN PUBLIKASI TUGAS AKHIR UNTUK KEPENTINGAN AKADEMIS

Sebagai sivitas akademik Universitas Indonesia, saya yang bertanda tangan dibawah ini:

Nama	: Rahardian Ghazali
NPM	: 0404840026
Program Studi	: S-1 Program Internasional
Departemen	: Teknik Metalurgi dan Material
Fakultas	: Teknik
Jenis Karya	: Skripsi

Demi pengembangan ilmu pengetahuan, menyetuji untuk memberikan kepada Universitas Indonesia **Hak Bebas Royalti Nonekslusif (Non-exclusive Royalti-Free Rights)** atas karya ilmiah saya yang berjudul:

EFFECT OF COOLING RATE AND TERNARY ADDITIONS OF CHROMIUM ON THE MICROSTRUCTURE OF TI-SI EUTECTIC ALLOY

Beserta perangkat yang ada (jika diperlukan). Dengan Hak Bebas Royalti Nonekslusif ini Universitas Indonesia berhak menyimpan, mengalihmedia/format-kan, mengelola dalam bentuk pangkalan data (database), merawat, dan mempublikasikan tugas akhir saya tanpa meminta izin dari saya selama tetap mencantumkan nama saya sebagai penulis/pencipta dan pemilik Hak Cipta.

Demikian pernyataan ini saya buat dengan sebenarnya.

Dibuat di : Depok
Pada tanggal : 17 Juli 2009
Yang menyatakan

(Rahardian Ghazali)

ABSTRACT

Name : Rahardian Ghazali

Study Program : Metallurgy and Materials Engineering

Title : Effect of Cooling Rate and Ternary Additions of Chromium on the Microstructure of Ti-Si Eutectic Alloy

This project investigates the effect of cooling rate and ternary additions of chromium (Cr) on the microstructure of a Ti-Si eutectic alloy. In doing so, three different samples with various composition were prepared, they are: Ti-8.5wt%Si (eutectic), Ti-8.5wt%Si-0.2wt%Cr, and Ti-8.5wt%Si-0.02wt%Cr. During the casting process of each specimen, the molten metal was poured into a wedge-shaped water-cooled copper mould so that they have a range of cooling rate along their length. A calibration curve to determine the cooling rates at different points along the mould was prepared using an Al-6.5wt% Si alloy, for which the relationship between Dendrite Arm Spacing and cooling rate is already known. Observation by using Scanning Electron Microscope (SEM) was also performed in order to observe the change in the lamellar spacing. And in order to relate the change in the lamellar spacing with the mechanical properties, the Ti specimens were subjected to Ball Indentation Test (BIT). The result shows that the relationship between the strength and the lamellar spacing in both Ti-Si eutectic and Ti-Si eutectic +0.02wt%Cr samples is a Hall Petch-like relationship, where the strength of the material increases with a decrease in lamellar spacing. However, the strength of these two specimens reaches its critical value when the lamellar spacing is about 240 nm. Further from this point, the strength decreases as the lamellar spacing becomes smaller. The result also shows that the dependency of strength on the lamellar spacing in Ti-Si+0.2wt%Cr is different with the other two samples in a way that there is a continual softening as the lamellar spacing becomes smaller. At this stage, the reason for this is still unknown, therefore, further investigation under TEM is required to observe the deformation mechanism in this particular sample.

Key words:

Ti-Si Eutectic, Ball Indentation Test (BIT), Lamellar Spacing

TABLE OF CONTENTS

LIST OF FIGURES

LIST OF TABLES

CHAPTER I
INTRODUCTION

I. 1. BACKGROUND

Titanium based alloys have been widely used in many fields such as petrochemical engineering, medical appliances, aerospace and many structural applications due to their low density, good creep performance, very high strength and toughness as well as excellent corrosion resistance. Titanium can exist in two crystal forms; alpha (α), which is a hexagonal close-packed structure and beta (β), which is body-centred cubic. The alpha structure is stable up to 883°C in pure titanium, and it transforms into the beta phase above this temperature. After transformed into beta phase, it will then remain stable up to the melting point. The reversible transformation of the crystal structure from alpha to beta when it exceeds certain temperature level becomes one of the important characteristics of titanium-base metals. This allotropic behavior depends on the type and amount of alloy contents, and it makes possible for complex variations in microstructure and more diverse strengthening opportunities than those of other nonferrous alloys such as aluminium and copper [1].

Figure 1.1. Titanium alloys capable of operating at temperatures from sub zero to 600°C are used in aircraft engines. Source: *http://www.msm.cam.ac.uk/phase-trans/2004/titanium/titanium2.html*

However, it is also well known that casting of titanium and its alloys has some inherent problems, notably, in the selection of mould material, severity of metal mould reactions, relatively low castability and high energy consumption. These

difficulties however, can be minimized by the development of low-melting cast eutectic alloys with appreciable mechanical properties. The majority of binary eutectic alloys of titanium are formed at high concentration (~25 – 40 wt%) with most of the elements [2]. Two elements with low density, Si and Be, form binary eutectics with titanium at lower concentrations (~8wt%). But, Ti-Be system has not received much attention due to the toxic nature of Be. The Ti-Si system however, has been investigated in some detail. The alloy system exhibits a eutectic reaction at a temperature of 1326 ^{o}C (1600 K) and 8.5 wt% Si and forms a lamellar eutectic structure upon cooling from the melt. However, the development of this alloy has been severely limited by its low room-temperature plasticity, induced by the essential brittleness of Ti_5Si_3 intermetallic compound. Many research papers has stated that it is possible to improve the ductility and toughness of this alloy by adopting minor addition of third element in order to modify their solidification behavior and microstructure [2].

I. 2. OBJECTIVES

The objectives of this present study are:

- To investigate the possibility of modifying Ti-Si eutectic structure with small additions of chromium
- To investigate the effect of cooling rate and ternary additions of chromium on the microstructure of Ti-Si eutectic alloy
- To investigate the relationship between lamellar spacing and mechanical properties in Ti-Si eutectic alloy.

I. 3. SCOPE OF RESEARCH

In the present study, three different samples with various composition were prepared, they are: Ti-8.5wt%Si (eutectic), Ti-8.5wt%Si-0.2wt%Cr, and Ti-8.5wt%Si-0.02wt%Cr. The specimens were solidified in a water-cooled copper mould having a wedge shape so that they have a range of cooling rate along their length. A calibration curve to determine the cooling rates at different points along the mould was prepared using an Al-6.5wt% Si alloy, for which the relationship between Dendrite Arm Spacing and cooling rate is already known. The microstructure of the samples was observed by

using optical microscope and Scanning Electron Microscope (SEM). In order to relate the change in lamellar spacing with the physical properties, the specimens were subjected to Ball Indentation Testing (BIT).

CHAPTER II
LITERATURE REVIEW

II. 1. *Basic Properties of Titanium*

High strength, low density, and excellent corrosion resistance are the main properties that make titanium attractive for a variety of applications. Examples include aircraft and its engine (high strength to density ratio and creep resistance up to about 550 ^{o}C), biomedical devices (corrosion resistance and high strength), and components in chemical processing equipment (corrosion resistance) [3].

Although titanium has the highest strength to density ratio, it is only applicable for certain niche application areas due to its high price that mainly a result of the high reactivity of this metal with oxygen. The use of inert atmosphere or vacuum is required during the production process of titanium sponge from titanium tetrachloride, as well as during the melting process, that results in an increase in the total production cost of this metal. On the other hand, the much higher melting temperature of titanium as compared to aluminum gives titanium a definite advantage when it is used in a temperature above 150 ^{o}C. However, the maximum use temperature of titanium alloys is mainly limited to about 600 ^{o}C by the high reactivity with oxygen. This is because above this temperature, the diffusion of oxygen through the oxide surface layer becomes too fast resulting in excess growth of the oxide layer and embrittlement of the adjacent oxygen rich layer of the titanium alloy. Table 2.1 shows us some of the basic properties of titanium as compared to those of other structural metallic material based on Fe, Ni, and Al [3].

Table 2.1 some important characteristics of titanium as compared to other structural metallic materials [3]

	Ti	Fe	Ni	Al
Melting Temperature (°C)	1670	1538	1455	660
Allotropic Transformation (°C)	$\beta \xrightarrow{882} \alpha$	$\gamma \xrightarrow{912} \alpha$	-	-
Crystal Structure	bcc → hex	fcc → bcc	fcc	fcc
Room Temperature E (GPa)	115	215	200	72
Yield Stress Level (MPa)	1000	1000	1000	500
Density (g/cm^3)	4.5	7.9	8.9	2.7
Comparative Corrosion Resistance	Very High	Low	Medium	High
Comparative Reactivity with Oxygen	Very High	Low	Low	High
Comparative Price of Metal	Very High	Low	High	Medium

II. 2. *Transition from Columnar to Equiaxed Growth (CET) during Solidification*

One of the most important routes to produce metals and alloys is the solidification process. During this process, the variations of temperature gradient and growth rate together with different alloy compositions lead to a multitude of microstructure, and hence, mechanical behavior. One of the important transitions that have to be precisely controlled is the so-called columnar-to-equiaxed transition (CET) [4]. This transition is usually assumed to occur when the advance of the columnar front is blocked by equiaxed grains that grow in the constitutionally undercooled liquid ahead of the columnar dendrites. CET has been reported to be sensitive to many of the parameters associated with the casting process, and these include the alloy composition, cooling rate, trace elements present in the melt, casting size and mould material. After the molten metal is poured into the mold, solidification starts at the cool mould walls and a solid shell will form quickly. The fastest heat transfer direction is along the mold walls. After the formation of the shell, the fastest heat transfer direction changes into the direction perpendicular to the wall from the liquid. Columnar structure grows along this direction and toward the melt until the growth is interrupted by central equiaxed grains [6].

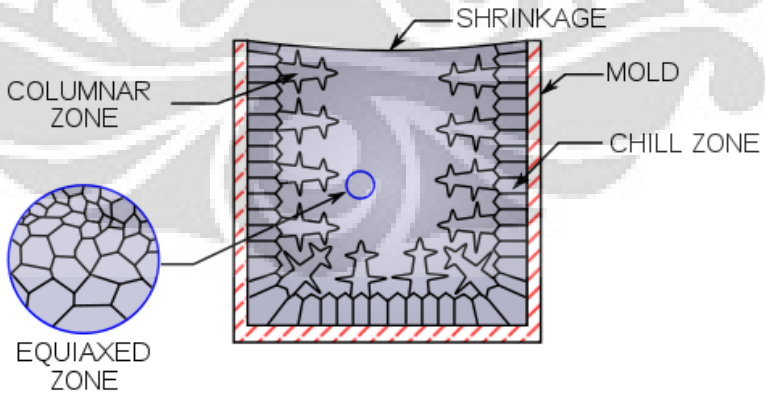

Figure 2.1. l zone. [5]

It is well known that the mechanical properties of castings and ingots are also determined by the columnar and equiaxed structures and its interfacial properties. In

order to maximize the mechanical properties of a casting product that is aimed for certain applications, some solidification processes make use of a close control of the CET either eliminating it or enhancing it [6].

II. 3. *Mechanical and Microstructural change induced by ternary additions*

The Ti-Si eutectic alloy has a strengthening mechanism that is very different from the traditional titanium alloys. The main difference lies on the fact that the Ti-Si eutectic system consists of a ductile phase (α-Ti which is the matrix) and brittle phase (Ti_5Si_3, acts as the reinforcement) [7].

$$(Ti\text{-}Si)_L \longrightarrow Ti + Ti_5Si_3$$

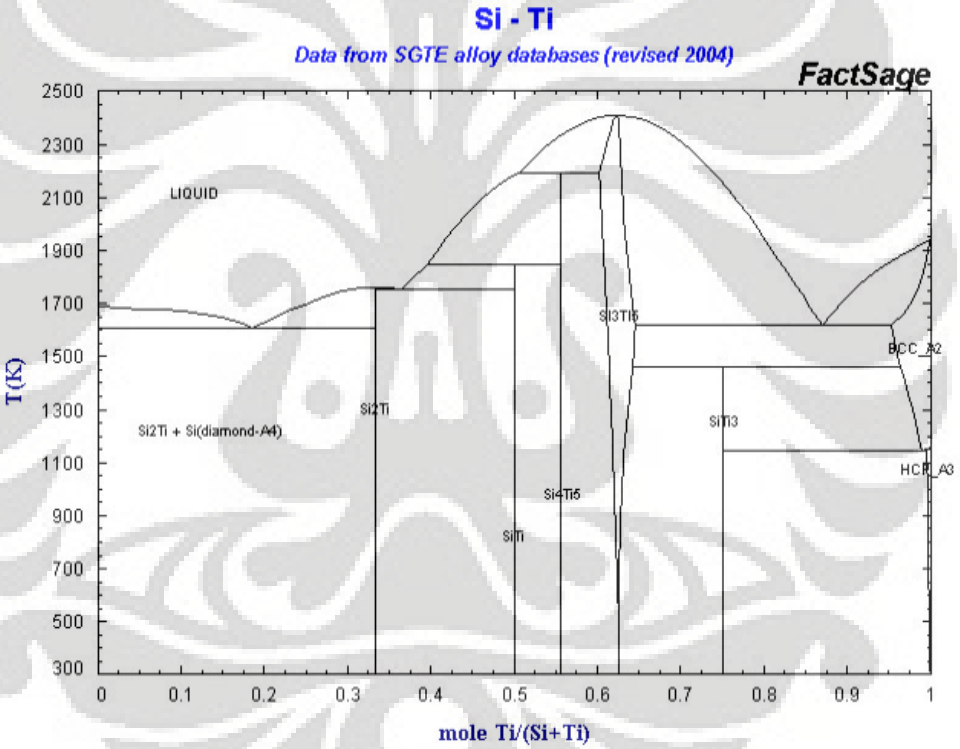

Figure 2.2. Si-Ti phase diagram [8]

However, as mentioned before, the development of this alloy has severely limited by its low room-temperature plasticity, induced by the essential brittleness of Ti_5Si_3 intermetallic compound. Researches on Ti-Si alloys have found that an increase in Si content lead to an increase in tensile strength and attains a maximum value of 750 MPa at 2 wt% Si. However, further addition of Si (up to 3wt%) resulted in a decrease in tensile strength to ~540 MPa. In addition, the alloys also exhibit very

low ductility (<0.1%) when the Si content exceeded more than 2wt%. More recently, a directionally solidified Ti-Si eutectic (8.5 wt% Si) alloy has found to exhibit a tensile strength as high as ~1000 MPa and elastic modulus of 190 GPa, but with almost zero ductility [7]. This alloy was thought to be an alloy of industrial importance provided its ductility could be improved. Table 1 below describes the tensile properties of Ti-Si alloy with various Si compositions.

Table 2.2 Tensile properties of Ti-Si alloys with various Si compositions [6]

Si (wt%)	UTS (MPa)	0.2% Yield Strength (MPa)	Elongation (%)
0	315	207	30
0.6	535	423	21
1.0	686	608	18
2.0	780	726	1
3.0	589	-	< 0.1
4.5	711	687	0.7
6.5	834	736	0.8
8.5	775	726	0.4

Ti-8.5wt%Si alloy forms a lamellar eutectic structure upon cooling from the melt. One of the main factors affecting the mechanical properties of a lamellar two-phase alloy is the spacing between the lamellae. Some literatures has pointed out that the Hall-Petch equation describes the relationship between yield stress (σ_y) and lamellar spacing (λ)

$$\sigma_y = \sigma_o + \frac{k}{\sqrt{\lambda}} \quad \text{..... (2.1)}$$

Where σ_o and k are materials constant. Based on the equation above, it is clear that one possible way to improve the mechanical properties (yield stress/hardness) of a lamellar two-phase alloy is by lamellar refinement. However, the ductility of this alloy will be decreased as the spacing between the lamellae becomes smaller, this is because more matrix/lamellae interfaces that act as a hindrance for dislocation movement are introduced to the system.

Minor addition of third element is usually adopted to increase the ductility and toughness of eutectic alloys by modifying their solidification behavior and microstructure. A good illustration in this regard is the modification of the Al-Si eutectic alloy by minor additions of Na or Sr [7]. According to the literatures, by considering the important role played by Na or Sr in modifying the microstructure of

an Al-Si eutectic alloy, attempts were made in order to increase the ductility of Ti-6.5wt%Si alloy by minor addition of low surface tension elements, namely, Na, Sr, Se, Te and Bi. It was found that the addition of these elements led to modification of microstructure with apparently no significant enhancement of tensile ductility, with exception of bismuth. The improved ductility in Ti-Si-Bi alloy is attributed to the change in the morphology of eutectic silicides which were finer and displayed reduced interconnectivity. In addition, the increase in the volume fraction of dendrites may also contribute to the enhanced ductility of the alloy [9].

Some literatures have also pointed out that large addition of Cr on Ti-Si system leads to a formation of quasicrystalline phase. Therefore, Cr obviously had an effect on the crystal structure. In this project, a small amount of Cr is added to Ti-Si system in order to find out if it is possible to modify the eutectic structure with small additions of Cr.

II. 4. *Pattern Formation in Solidification*

According to *Science and Technology of Advanced Materials 2 (2001) 147-155*, Regular patterns form in a number of solidification processes. Examples occur during lamella and rod-like eutectic growth and when single phase cells or dendrites are formed. As a lamella eutectic grows, different amounts of solute are deposited in the two solid phases. At steady state, concentration gradient build up to transport the solute across the lamella. The concentration gradient in the liquid near the solid means that if the effect of surface energy is neglected, the interface could not be at local equilibrium at more than one point. By considering the effect of curvature on the melting temperature and adjusting the interface shape, it is possible to satisfy local equilibrium at all points on the solid-liquid interface [10].

In directionally grown peritectics, the pattern and scale of the microstructure are usually determined by the cells or dendrites of the high-temperature phase. In each of these examples, the scale of the microstructure can control later reactions and eventual properties of the material. J.D. Hunt on one of his paper stated that steady-state analysis indicates that a wide range of possible spacings could occur during eutectic, cellular or dendritic growth. The degree of freedom is

removed by considering the mechanism determining the minimum and maximum spacing on the specimen. it is found that the minimum spacing occurs when the array first becomes stable for a lamella or rod-like eutectic, for cell growth and for some dendrites. For low temperature gradient, high velocity dendrites, the minimum spacing is determined by the spacing when the dendrites first become near enough to interact. The maximum spacing for eutectics and for cells is determined by tip splitting. The maximum spacing for dendrites occurs when tertiary arm becomes a new primary [10].

CHAPTER III
EXPERIMENTAL METHOD

III. 1. FLOW CHART OF THE PROJECT

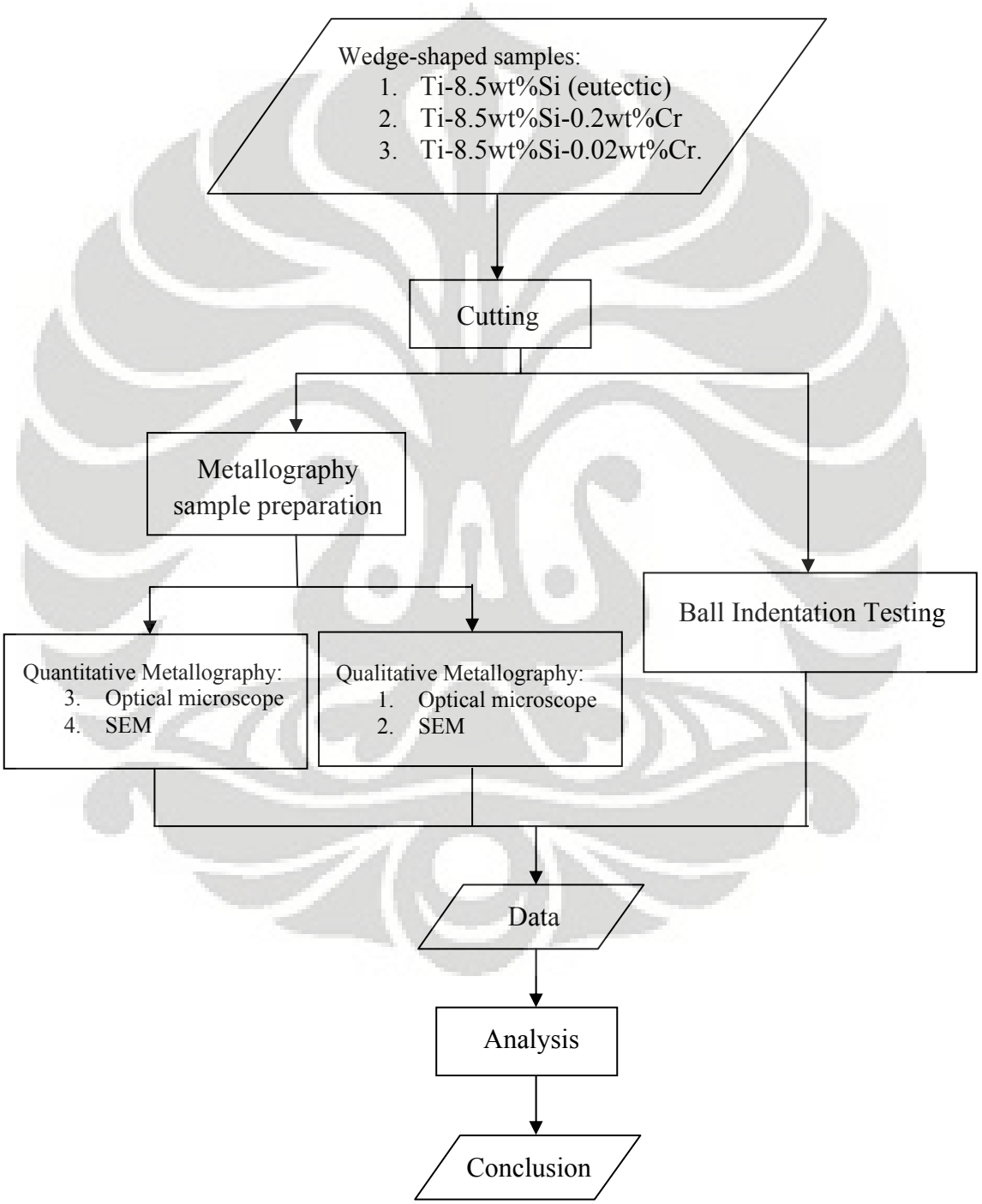

III. 2. MATERIALS AND EQUIPMENTS

3. 2. 1. Materials

- Samples: 1. Ti – 8.5wt% Si (eutectic)
  2. Ti – 8.5wt% Si – 0.02wt% Cr
  3. Ti – 8.5wt% Si – 0.2wt% Cr
- Silicon-carbide grinding paper
- Polishing cloth
- Dilute aqueous solution containing HF and HNO3 (Kroll reagent for the etchant)
- Ethanol
- Kerosene
- Epofix hardener
- Epofix resin
- Colloidal Silica Suspension

3. 2. 2. Equipments

- Buehler slow speed cutting saw
- Plastic mold for cold mounting
- Struers grinding machine (alumunium samples)
- Struers polishing machine (alumunium samples)
- Struers automatic polishing and grinding machine (titanium samples)
- Spray gun
- Ultrasonic bath for the removal of surface contaminants
- Optical microscope
- Olympus optical micrograph
- Ball Indentation Testing Machine (Mini Instron)
- Scanning Electron Microscope (PHENOM)

III. 3. TESTING AND OBSERVATION

3. 1. Casting of the Samples

The Ti-Si and Ti-Si-Cr samples were prepared by melting the alloy in a non-consumable arc melting furnace. Each specimen was melted 4 times to ensure uniform chemistry of the alloy. The molten alloys were then poured into a water cooled mould having a wedge shape as shown in figure 3.2 (a). In order to get a wider range of cooling rate, each composition was made into two samples with different dimensions:

(a). Thin

Length : 35 mm
Width : 3 mm
Thickness : 9.2mm

(b). Thick

Length : 35 mm
Width : 6.2 mm
Thickness : 9.2 mm

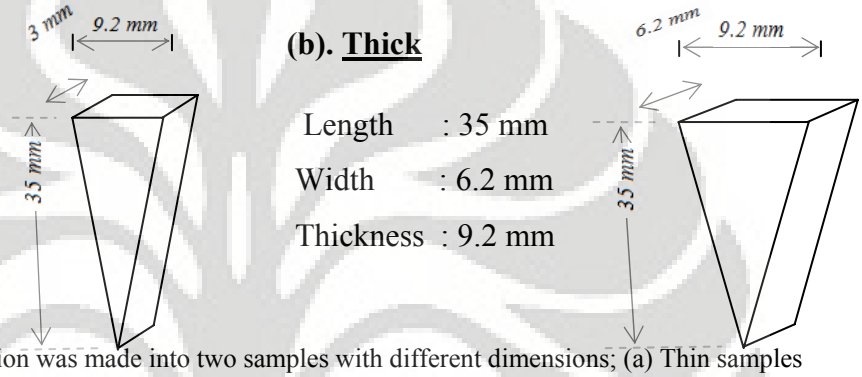

Figure 3.1. Each composition was made into two samples with different dimensions; (a) Thin samples and (b) Thick samples.

After cooled, the samples had small amount of excess metal on the top of them as shown in figure 4.b. The next step was removing these excess metals, followed by cutting the samples into two halves, so that we are able to examine the microstructure of the middle part. Due to the difference in the mould wall thickness, the specimens will have a range of cooling rates along their length. To simplify the identification of the positions, the samples were divided into 5 points along their length, where the distance between each point is approximately 7 mm. The Al-6.5wt%Si alloy was prepared in the same way.

Figure 3.2. (a) samples were casted in a water-cooled mould having a wedge shape, (b) cutting of the excess metal, (c) samples are cut into two halves, (d) range of cooling rate along the length of the specimens.

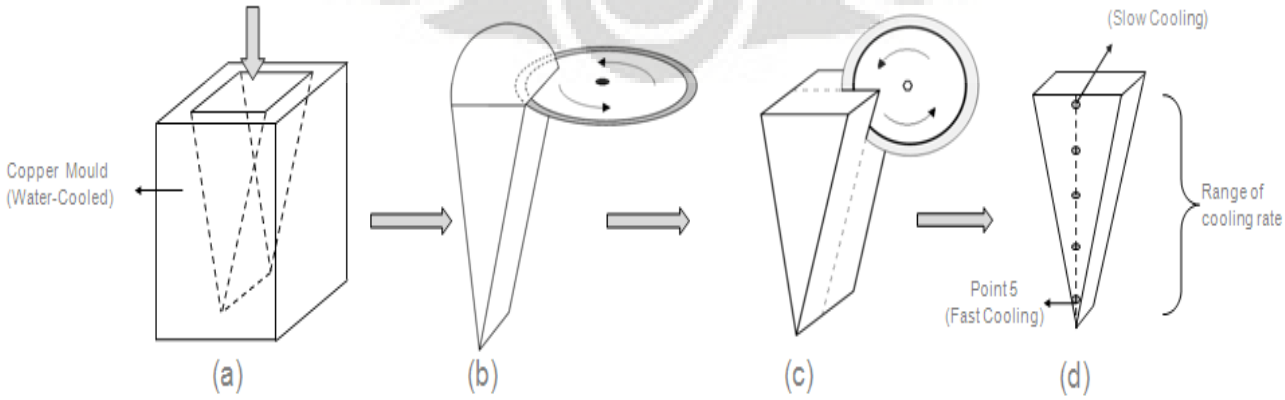

3. 2. *Metallographic Sample Preparation*

The samples were then mounted in epofix resin, followed by grinding, polishing and etching stages to allow examination under optical microscope. The Ti samples were etched with dilute aqueous solution containing HF and HNO3 (Kroll reagent). However, the Al samples were not etched because the microstructure was able to be examined after the polishing stage. The images of the microstructure in each point were taken and the effect of cooling rate was investigated

3. 3. *Determination of Cooling Rate*

Determination of cooling rate in the selected locations were done by calculating the Average Dendrite Secondary Arm Spacing of the Al-6.5wt%Si specimen, which has the same geometry as the Ti samples. The dendrite secondary arm spacings (λ) were measured as a function of the distance from the bottom of the Al-6.5wt% Si sample. Based on the ASTM E112 (test methods for determining the average grain size), λ can be estimated by counting the number of arms intercepted by one or more straight lines sufficiently long to yield at least 50 intercepts. To calculate the λ, following equations are used [11]:

$$\lambda = 359.52e^{-0.3468 \times G} \quad \text{..... (2.2)}$$

Where: G / ASTM grain size = $(6.643856 \log_{10} P_L)-3.288$ ..... (2.3)

$$P_L = \frac{Number\ of\ Arms}{Length} \quad \text{..... (2.2)}$$

In relation with cooling rate, the secondary arm spacing in Al-6.5wt% Si has been found to obey [12]:

$$\lambda = 50 \times 10^{-6} \left(\frac{dT}{dt}\right)^{-0.33} \quad \text{..... (2.4)}$$

Therefore, once we know the λ, the cooling rates can be determined by using this equation:

$$\left(\frac{dT}{dt}\right)^{-0.33} = \frac{\lambda}{50 \times 10^{-6}} \quad \text{..... (2.5)}$$

3. 4. *Observation under SEM (Scanning Electron Microscope).*

After observation under optical microscope, the etched samples were then separated from its mounting resin. Since the Phenom (SEM) can only observe samples with length less than 20 mm, the samples were then cut into two halves. SEM is required to observe the changes in morphology of the lamellar structure, since the magnification of the optical microscope is not sufficient to do the job.

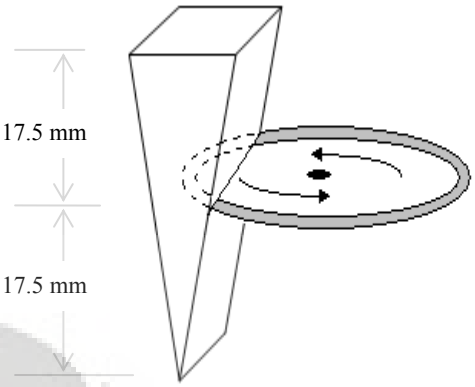

Figure 3.3. The samples were cut into two so that it can fit into the Phenom's sample holder

3. 5. *Mechanical Behavior (Ball Indentation Test)*

In order to relate the change in microstructure with the mechanical properties, the Ti samples were subjected to Ball Indentation Test (BIT). The basic principle of this technique is multiple indentations by a spherical indenter at the same test location on the test sample with intermediate partial unloading. Here a spherical ball with a specific rate of loading indents the test materials and 8 indentations in a single position is made through loading-unloading sequences [13]. The Ball Indentation Test was only performed up to point 4 in thick samples, whereas in thin samples, it was performed only in point 1, 2 and 3. This is because the surface area in the region close to the end of the sample is too small for BIT to take place. The consequence of performing BIT in these small areas is an inaccurate result that might be caused by the size of plastic zone is larger than the surface area as illustrated in figure below.

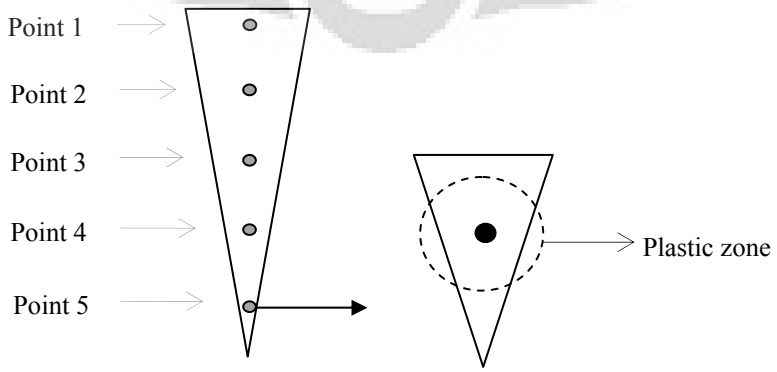

Figure 3.4. BIT cannot be performed in area close to the end of the sample because the plastic zone might be larger than the surface area, resulting in an inaccurate result.

The data obtained from the BIT was in the form of load vs extension curve of the 8 cycles as shown in figure below.

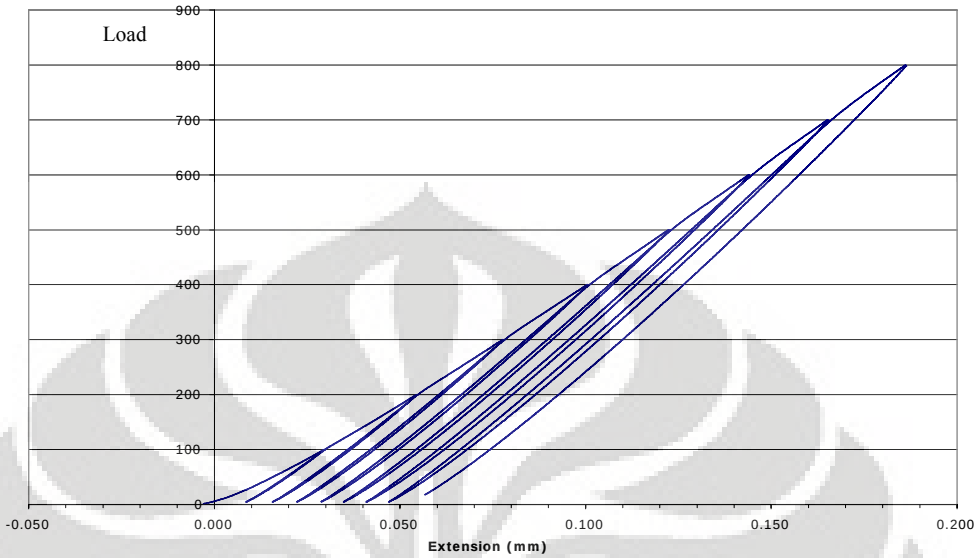

Figure 3.5. Example of load vs extension curve of the 8 cycles that is obtained from BIT

After we get the graph, each load/unload cycle was analyzed and three parameters were collected from the graph, which are:

- W, the peak load in Newtons
- h_t, the total extension (mm)
- h_p, the plastic extension (mm).

Figure 8 is an example of load vs extension curve of a single cycle that is obtained from ball indentation testing. The way of obtaining each parameter is described in this graph.

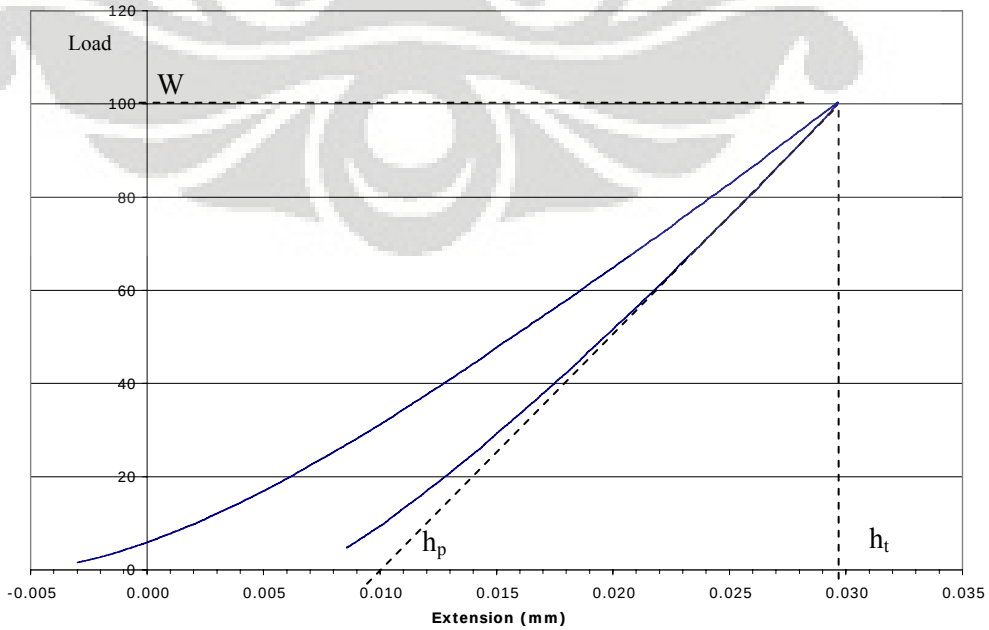

Figure 3.6. A curve of a single cycle, showing the three parameters to be determined.

After the three parameters were obtained, the stress and strain for each cycle can be calculated by using formulas below:

$$h_c = h_t - 0.75(h_t - h_p) \quad \text{.....} \quad (2.6)$$

$$a^2 = \frac{5(2-n)\,(2Rh_c - h_c^2)}{2(4+n)} \quad \text{.....} \quad (2.7)$$

$$\text{Stress} \rightarrow P_m = W/\pi a^2 \quad \text{.....} \quad (2.8)$$

$$\text{Strain} \rightarrow \varepsilon = 0.2a/R. \quad \text{.....} \quad (2.9)$$

Where R is the radius of the indenter, n is the work hardening coefficient and a is the contact radius between the indenter and the specimen's surface. The work hardening coefficient (n), is obtained by iteration.

After the value of stress and strain for each cycle is calculated, then it is plotted into a curve, where the strengthening factor and work hardening coefficient of the specimen in each point can be obtained by fitting a power law equation into the curve. An ***example*** of the stress-strain curve is given in figure below.

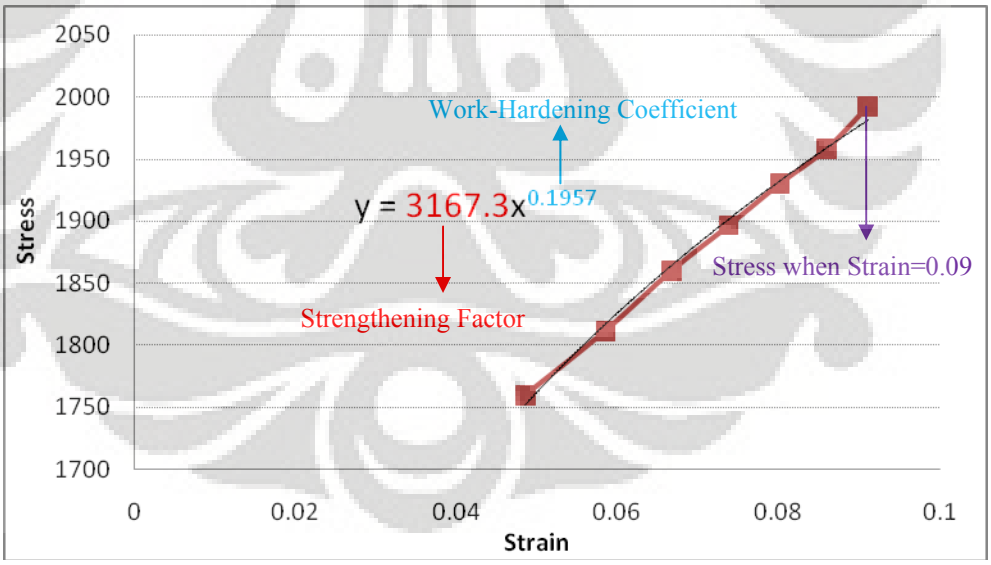

Figure 3.7. Power law equation is fitted into the stress-strain curve to obtain the strengthening factor and the work hardening coefficient.

After the strengthening factor and the work hardening coefficient are obtained for each point, they are then plotted into a curve against the lamellar spacing. The

magnitude of stress when the strain is equal to 0.09 is also obtained from the graph to estimate theoretical UTS. The power law equation is used to calculate the value of stress when the strain is equal to the work hardening coefficient. These results are shown in figures 4.16 to 4.18.

CHAPTER IV
RESULTS AND DISCUSSIONS

IV. 1. Determination of Cooling Rate.

After the Aluminium samples were cut into two halves, the photographs of the microstructure were taken in 6 different points along their length. Figure 4.1 illustrates the position of each point while figures 4.2 and 4.3 show the microstructures at the different positions for thick and thin samples.

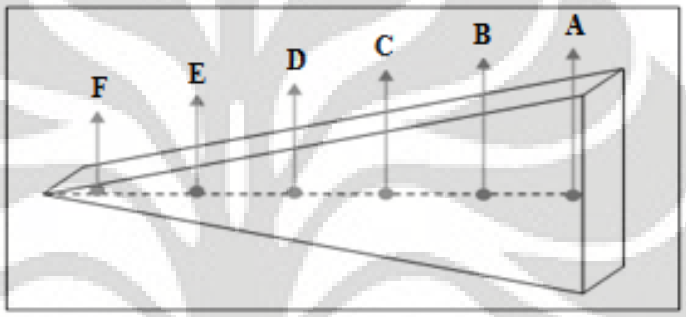

Figure 4.1. *Photographs were taken in 6 different points along the specimen's length*

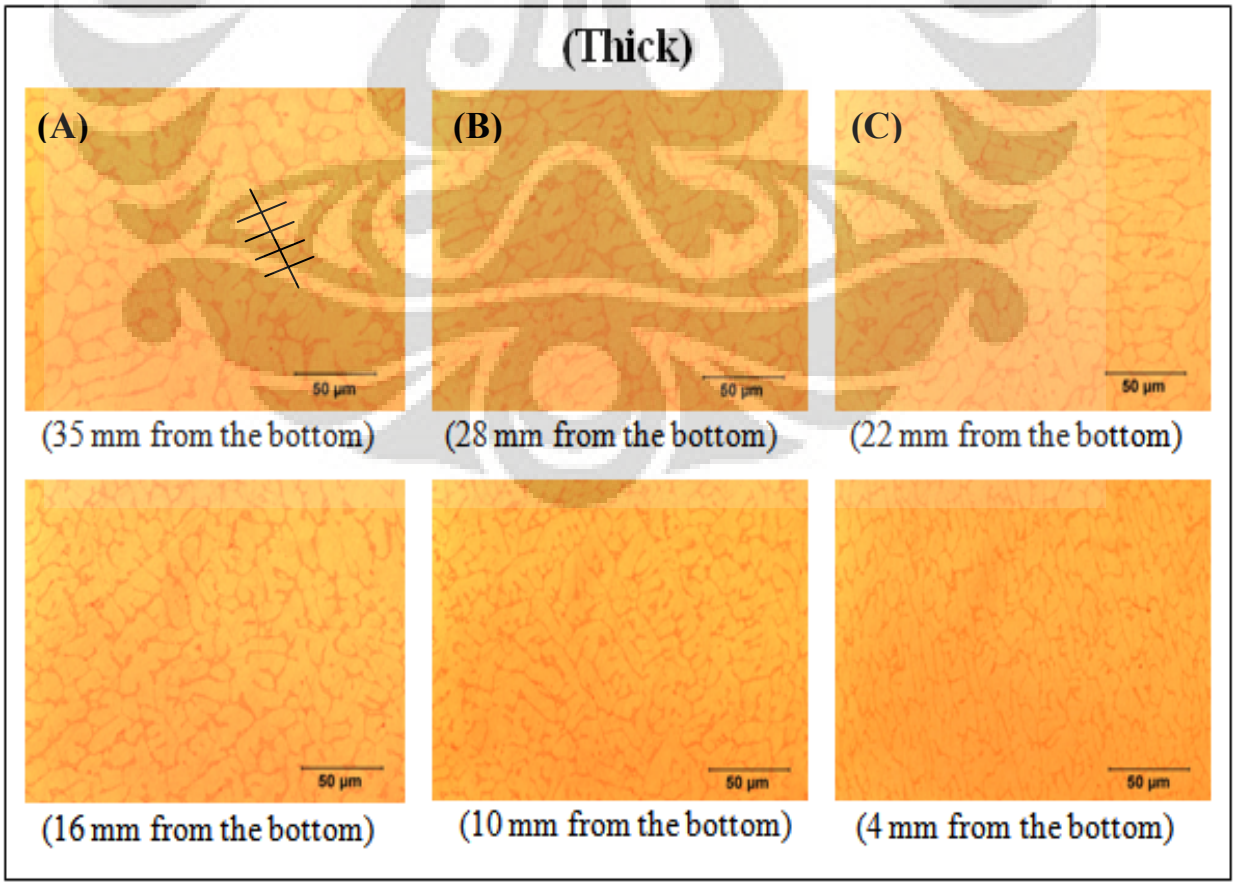

Figure 4.2. *Microstructure of the thick Al sample in 6 different points.*

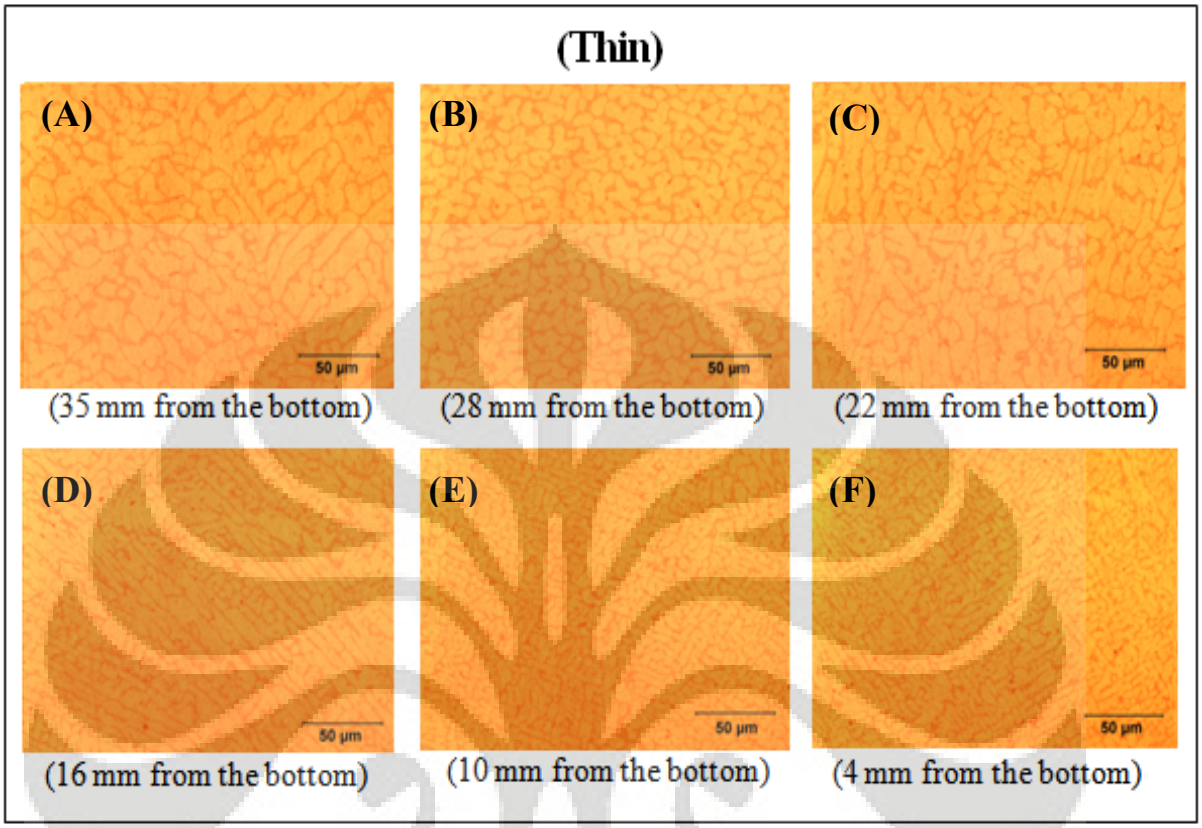

Figure 4.3. *Microstructure of the thin Al sample in 6 different points.*

As explained in the previous section, the cooling rate was determined by calculating the average secondary dendrite arm spacing of the aluminium sample, the smaller the dendrite arm spacing means the higher the cooling rate. The pictures above show us that as the distance from the bottom of the sample increases, the secondary dendrite arm spacing becomes larger. This is an indication that the thicker section of the specimen has slower cooling rate. The Al-6.5wt%Si was used to determine the cooling rate because the relationship between cooling rate and the microstructure (secondary dendrite arm spacing) is well characterized in many literatures. In addition, due to the shape and the dimension of the mould, we cannot put thermocouple to measure the cooling rate directly during the solidification process. It must be noted that the cooling rate of the Al samples is not exactly the same with those experienced by the Ti alloys, due to the difference in thermal conductivity (heat transfer) between Ti and Al, but the trend will be the same

because they have the same shape and dimension. Since we only want to get a general idea of how the cooling rate changes in every point along the length of the sample, we can plot a calibration curve by assuming that the highest cooling rate achieved by the aluminium sample is equal to 1.

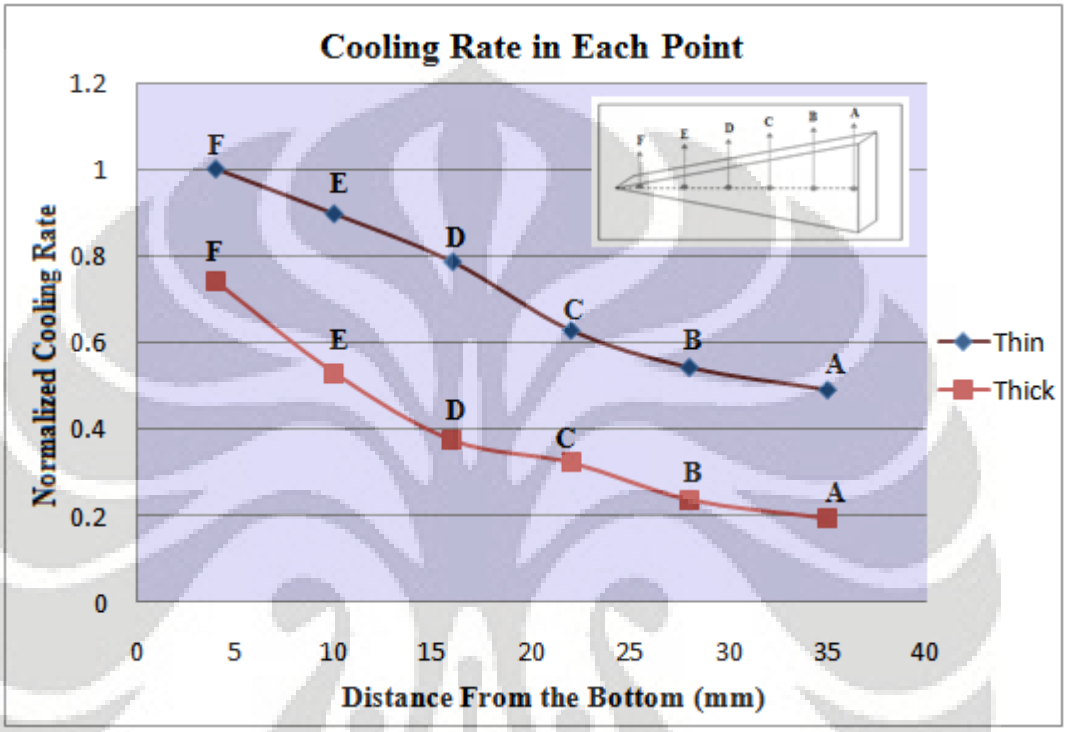

Figure 4.4. Calibration curve showing how the cooling rate changes as the specimen becomes thicker. The cooling rate in the thinnest section of the specimen (point F) is the highest compared to other points.

IV. 2. Microstructure

Each Ti sample was divided into 5 points along their length where the distance between each point is approximately 8mm. Photographs showing the microstructures of the samples with 5 and 20 times magnifications were taken in these points by using optical microscope. In addition to this, the SEM pictures with 15.000 times magnifications were also taken to observe the change in the lamellar spacing.

✓ Ti-Si eutectic (Thin)

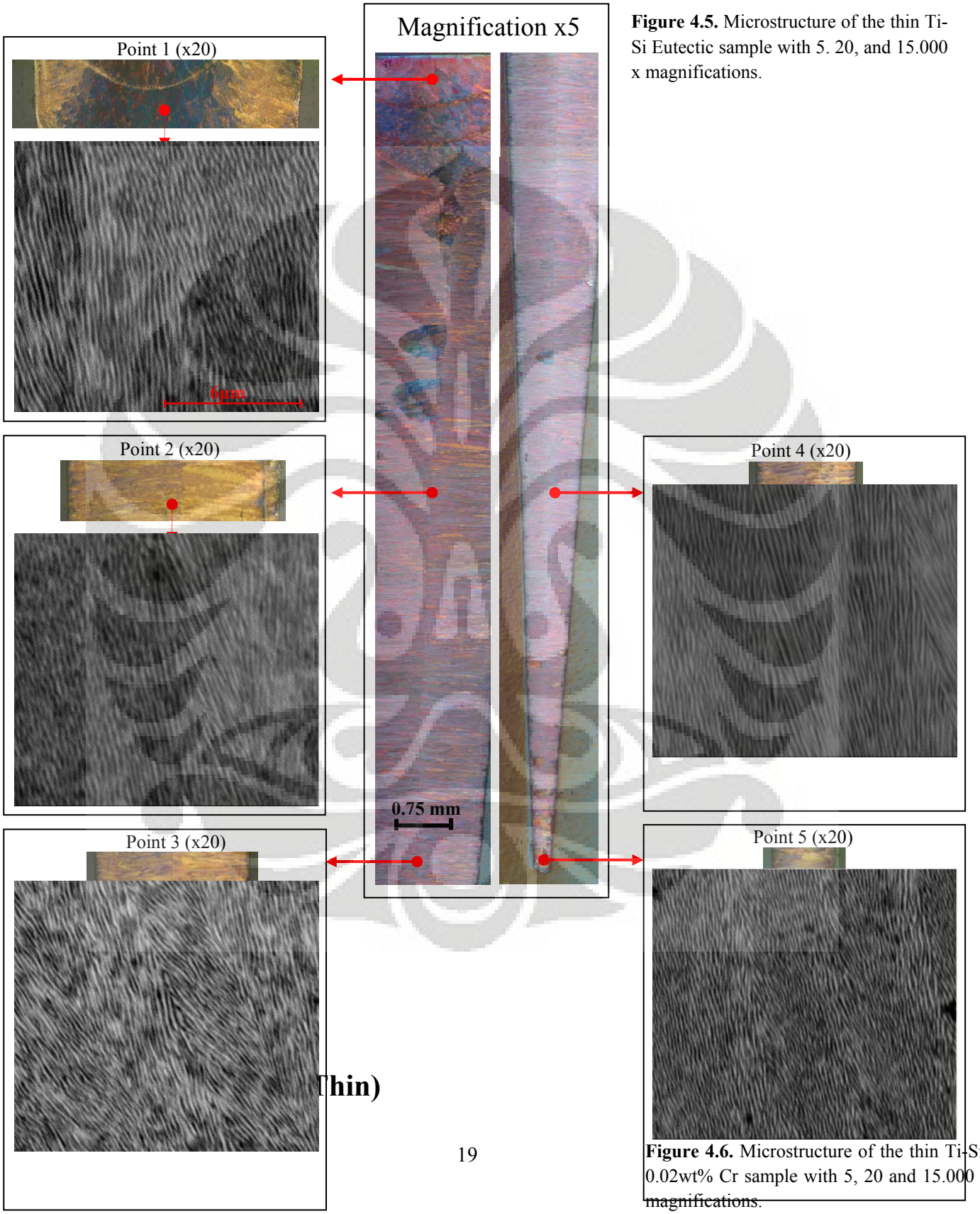

Figure 4.5. Microstructure of the thin Ti-Si Eutectic sample with 5. 20, and 15.000 x magnifications.

Figure 4.6. Microstructure of the thin Ti-Si-0.02wt% Cr sample with 5, 20 and 15.000 x magnifications.

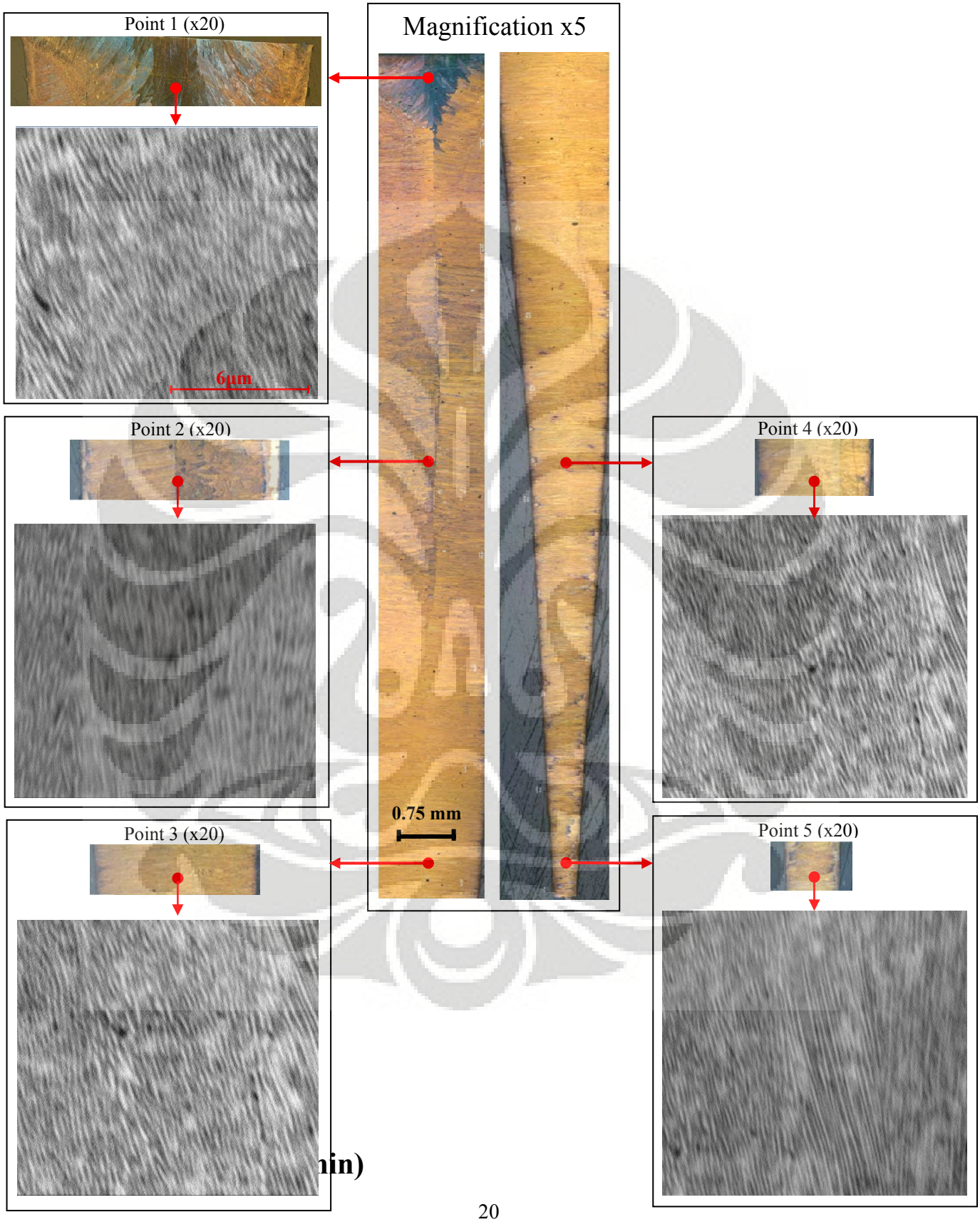
Point 1 (x20)
6µm
Magnification x5
0.75 mm
Point 2 (x20)
Point 4 (x20)
Point 3 (x20)
Point 5 (x20)

in)

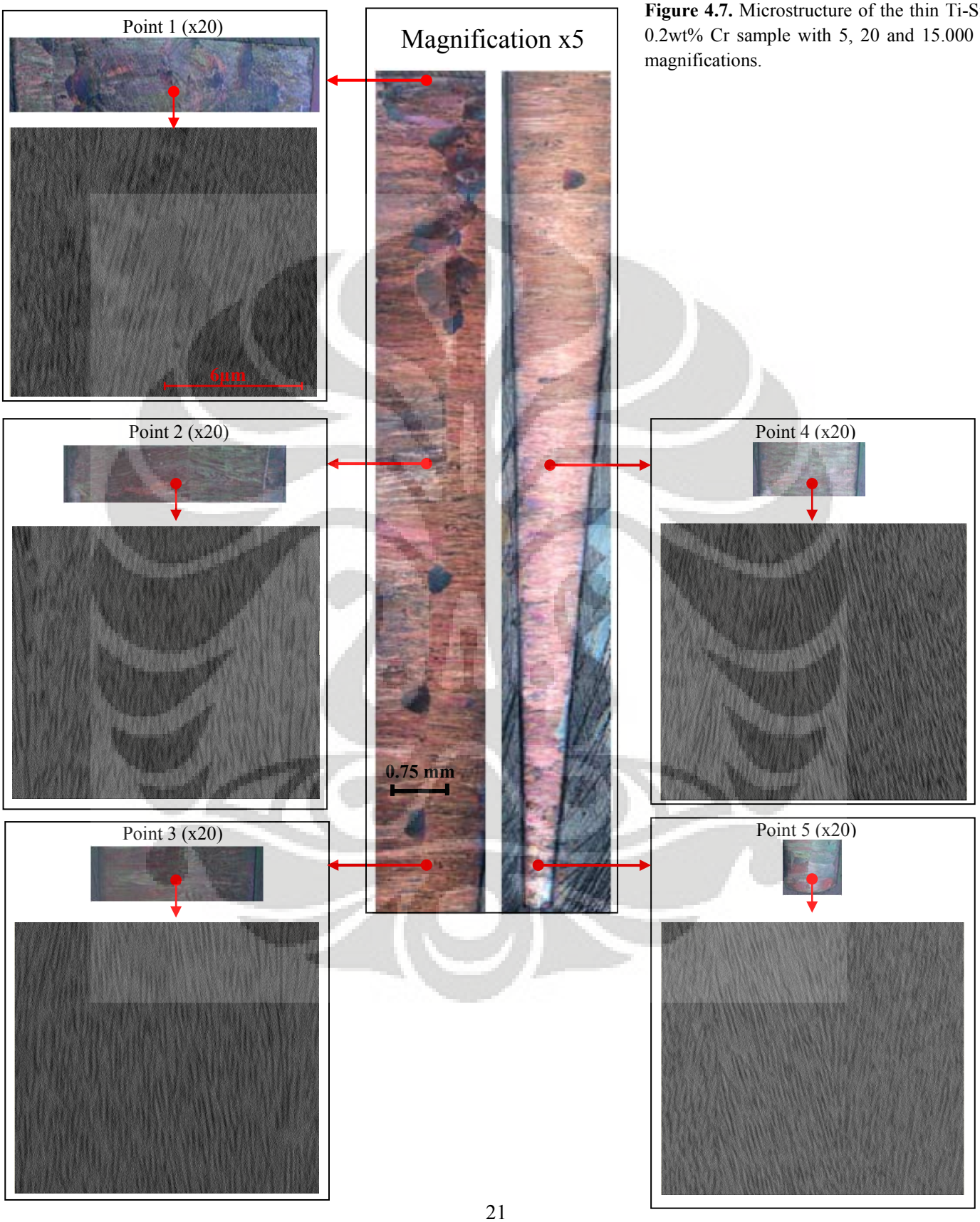

Figure 4.7. Microstructure of the thin Ti-Si-0.2wt% Cr sample with 5, 20 and 15.000 x magnifications.

✓ Ti-Si eutectic (Thick)

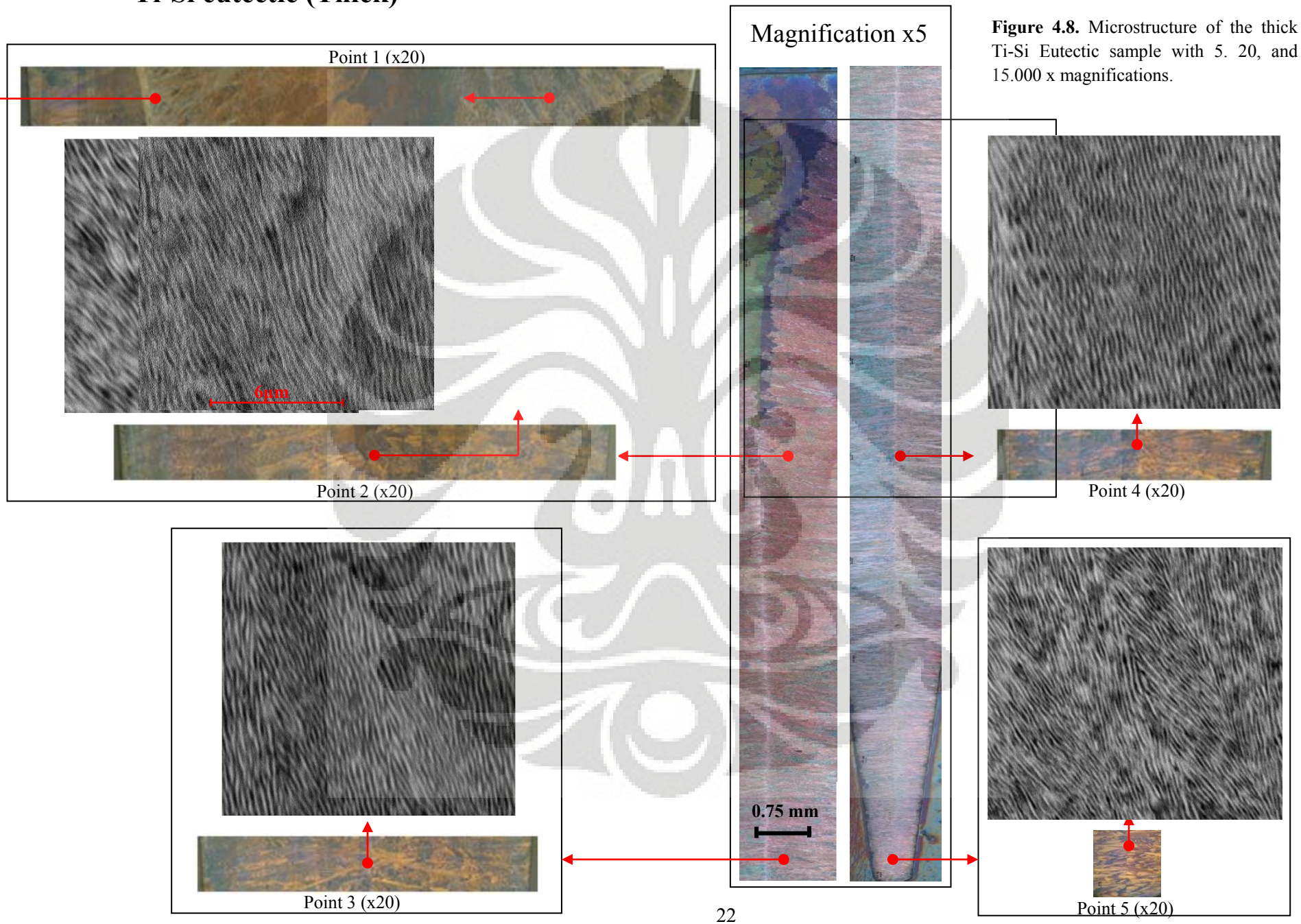

Figure 4.8. Microstructure of the thick Ti-Si Eutectic sample with 5. 20, and 15.000 x magnifications.

✓ Ti-Si-0.02wt% Cr (Thick)

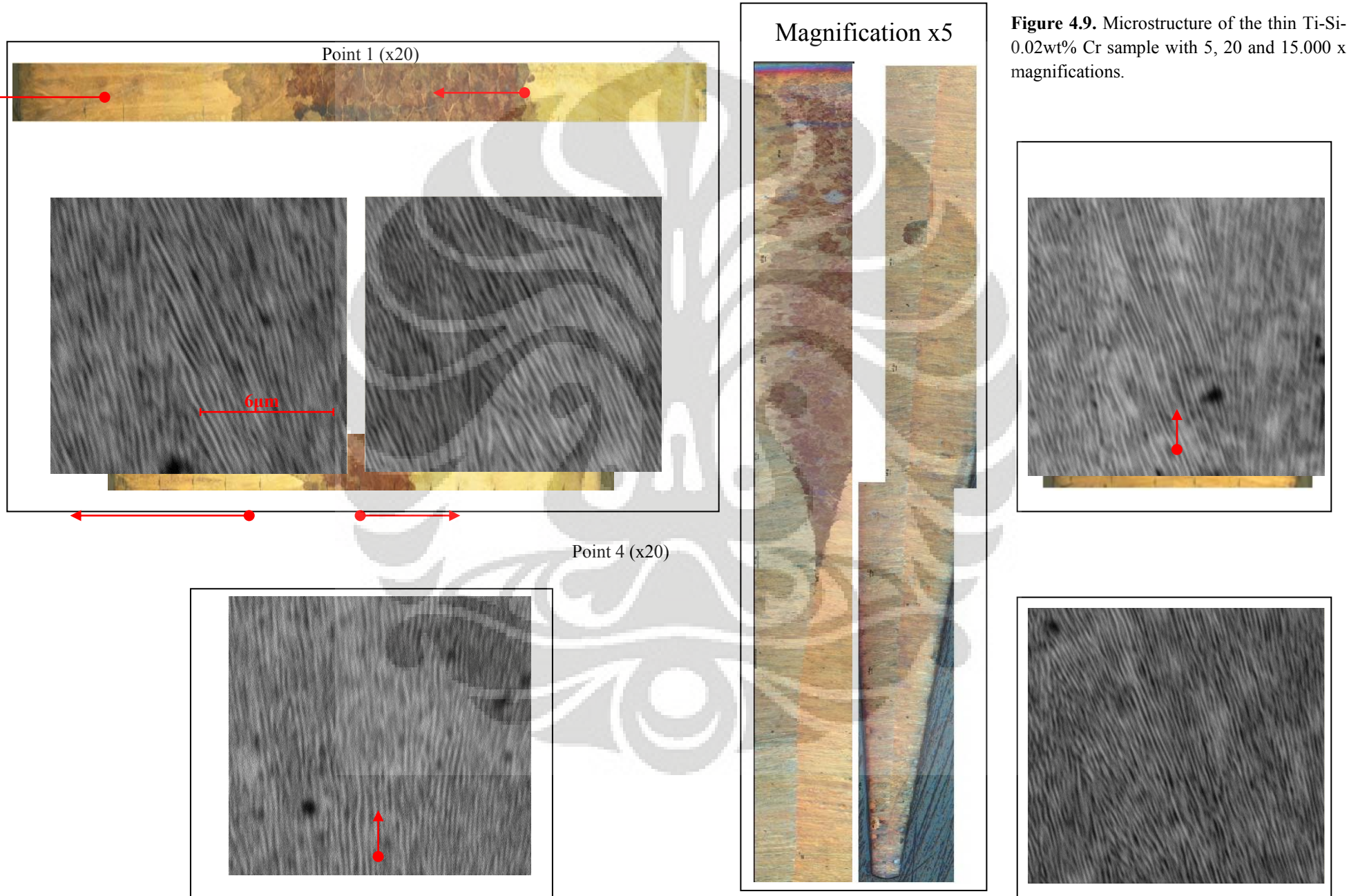

Figure 4.9. Microstructure of the thin Ti-Si-0.02wt% Cr sample with 5, 20 and 15.000 x magnifications.

✓ **Ti-Si-0.2wt% Cr (Thick)**

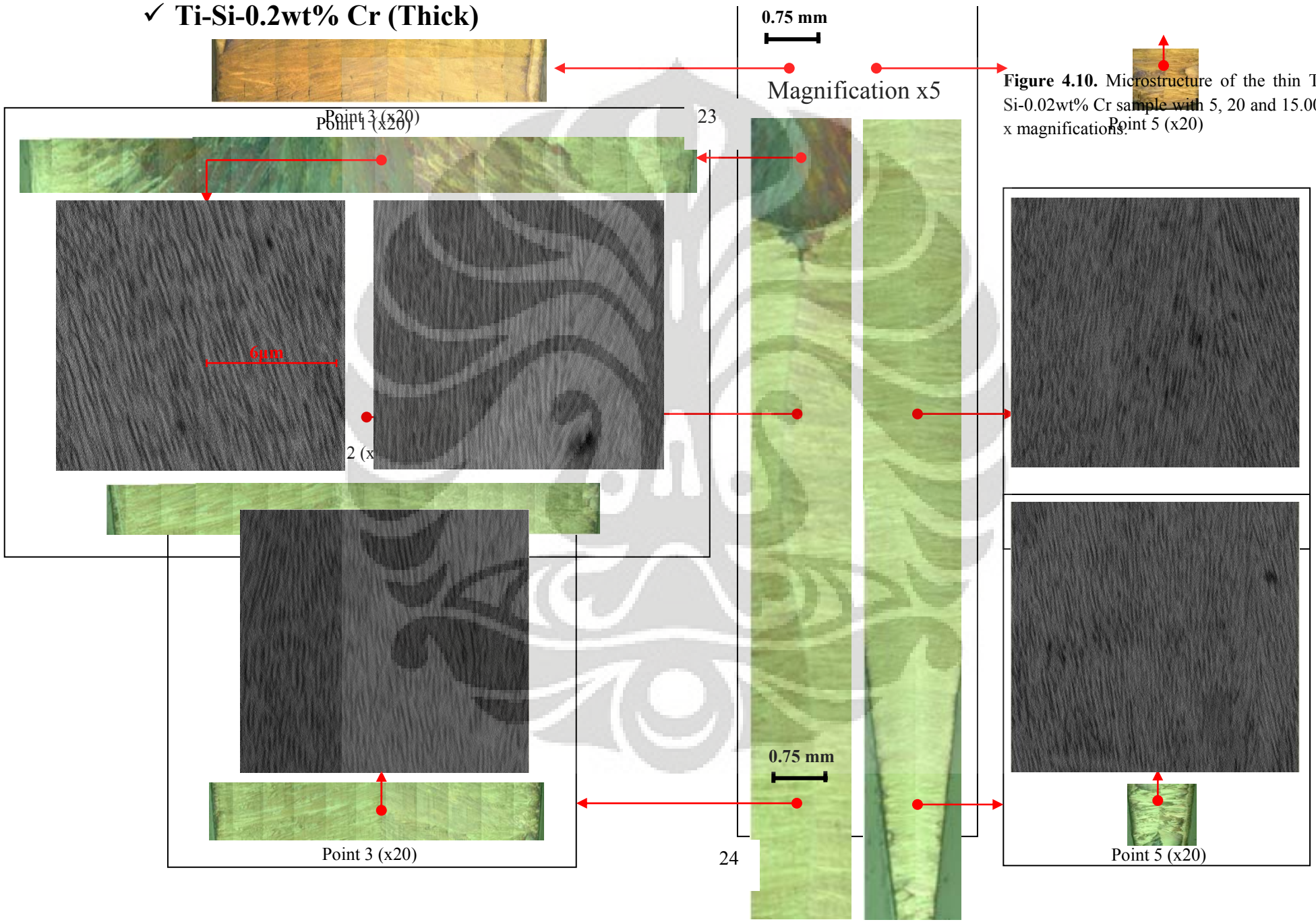

Figure 4.10. Microstructure of the thin Ti-Si-0.02wt% Cr sample with 5, 20 and 15.000 x magnifications.

After the SEM pictures showing the microstructure of all samples were obtained, the lamellar spacings were then measured and the result is plotted into a graph versus the cooling rate:

➢ **Ti-Si Eutectic**

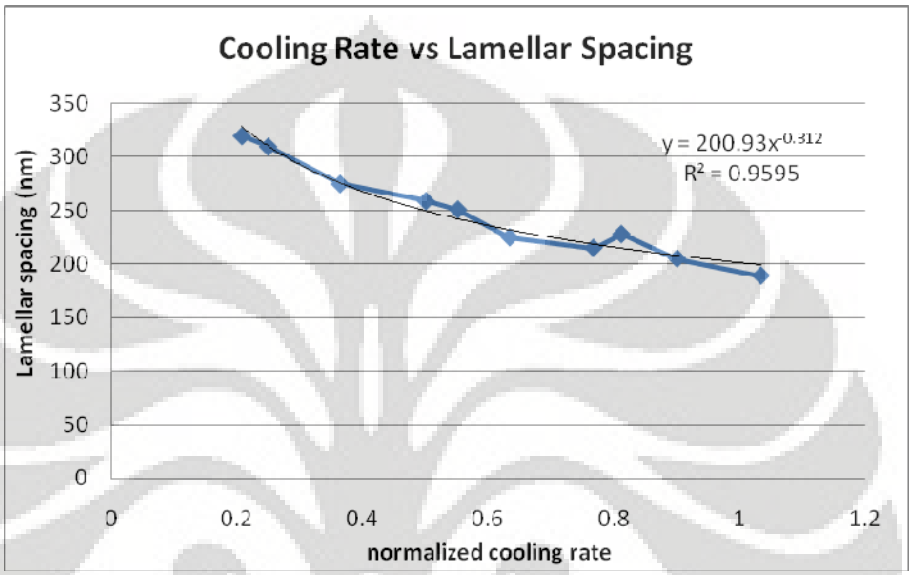

Figure 4.11. Relationship between the cooling rate and the lamellar spacing in Ti-Si eutectic

➢ **Ti-Si Eutectic + 0.02wt%Cr**

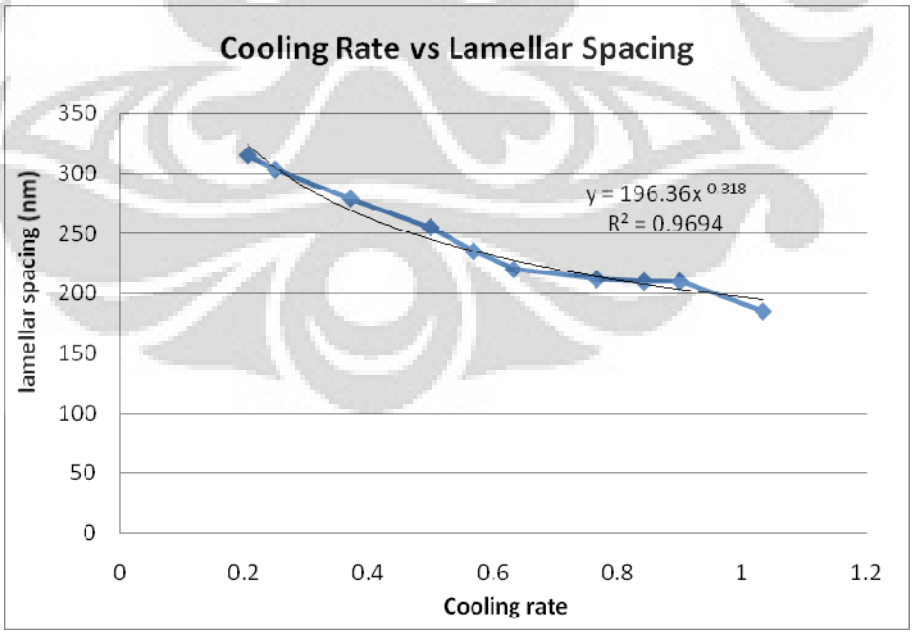

Figure 4.12. Relationship between the cooling rate and the lamellar spacing in Ti-Si+0.02wt%Cr

➢ **Ti-Si Eutectic + 0.2wt%Cr**

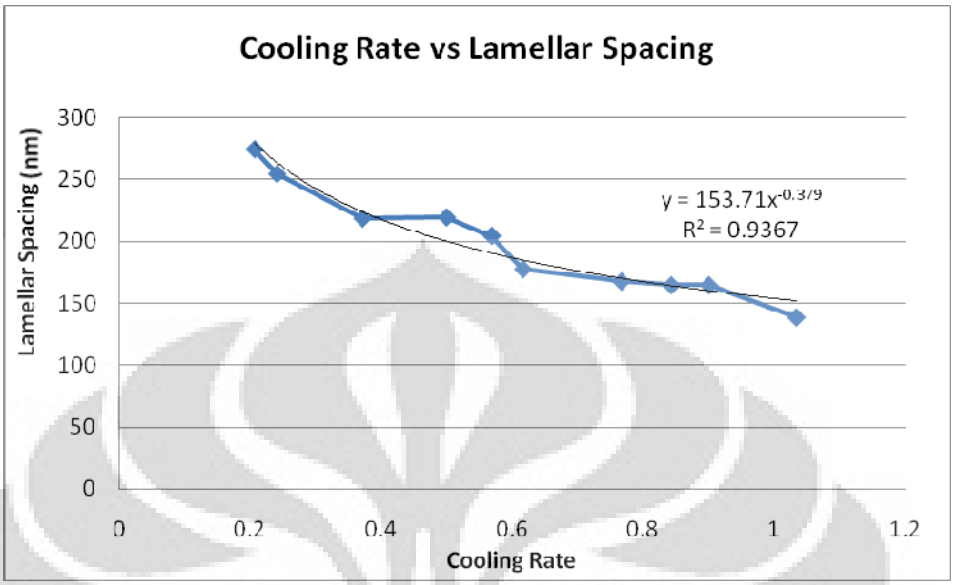

Figure 4.13. Relationship between the cooling rate and the lamellar spacing in Ti-Si+0.2wt%Cr

From the graphs above, it can be concluded that the cooling rate obviously had an effect on the lamellar spacing, where higher cooling rate leads to a refinement in the spacing between the lamellae. Figure 4.14 shows us the microstructure of the upper half of the three thick Ti samples. From the figure, it can be seen that there are two different zones present on the microstructure. The first zone, which is located in the area close to the metal/mould interface where the cooling rate is relatively high, is the columnar zone. And the second zone, which is the last zone to solidify, is the equiaxed zone. This zone is located in the centre of the thickest section of the specimens, where the cooling rate is relatively low. The main difference between these two zones is that the lamellae in columnar zones are having their preferential growth direction oriented parallel to the heat extraction, whereas in equiaxed zones the orientation of the lamellae is different in each grain. When we compare the microstructure of the three Ti samples, it is found that the Cr content had an effect on the size of the equiaxed zones, where further addition of Cr up to 0.2wt% leads to a reduction in the size of this zone. We can also see from the figures that the sizes of the equiaxed zones in thick samples are larger than in thin samples. This is attributed to the difference in cooling rate where according to the calibration curve, the cooling rate in thick samples is much slower

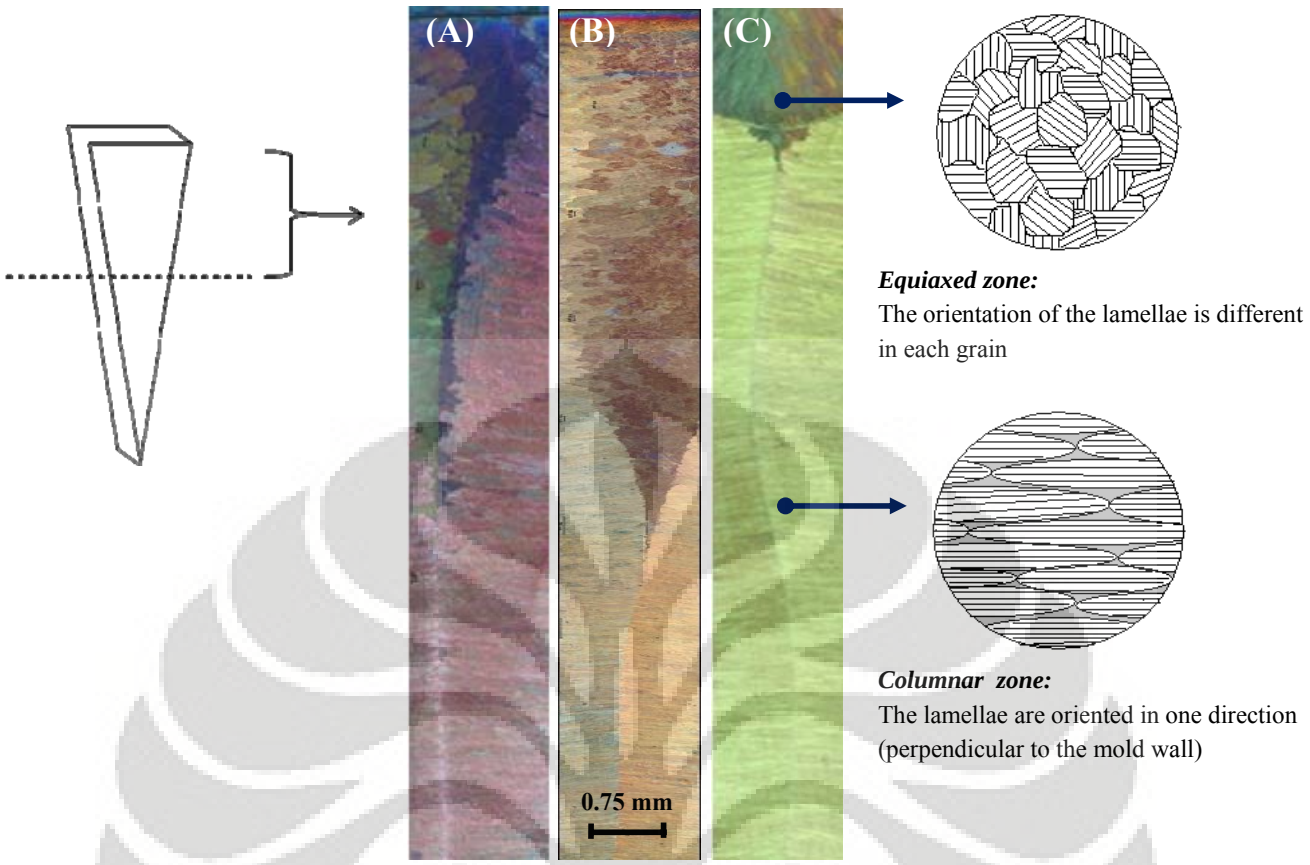

Figure 4.14. Microstructure of the three thick Ti samples taken with 5x magnification; (a) Ti-Si eutectic, (b) Ti-Si eutectic + 0.02wt%Cr and (c) Ti-Si + 0.2wt%Cr

The columnar-to-equiaxed growth (CET) is usually assumed to occur when the advance of the columnar front is blocked by equiaxed grains that grow in the constitutionally undercooled liquid ahead of the columnar dendrites. The main parameters that influence the CET include the cooling rate and the alloy composition. During the solidification of the samples, columnar crystals were started to grow fairly rapidly from the mould wall into an initially steep temperature gradient produced by the superheat liquid [6]. As the solidification proceed towards the centre, the temperature gradient in the liquid decreases because of the low thermal conductivity of titanium. And when the temperature gradient ahead of the columnar interface is low enough, equiaxed crystals were started to grow in the liquid. In some part of the specimens, the columnar structures progressed to the centre, where the grains advancing from the opposite wall meet. This is because during the solidification, the temperature gradient ahead of the columnar interface is still relatively high, and the fastest heat transfer is still in the direction perpendicular to the mould wall from the liquid even until the columnar grains growing from the opposite wall meet.

Observation under optical microscope reveals that some small dark areas similar to the shape of an equiaxed grains appear on the solidification line in thin Ti-0.2wt% Si sample. It has to be noted here that it is difficult to reach a 100% a compositional uniformity in a casting product. Therefore there is a possibility that these small zones are the area where the composition is different. However, in order to prove this theory, further investigation by using TEM (chemical analysis) is required. Another possibility is that these dark areas are an actual equiaxed grains that exist because many fine crystals were formed near the chilled zone, and some of these small crystals may be transported by fluid convection to the centre of the casting where they act as preferred sites for grain growth.

In order to observe the effect of ternary addition of Cr on the morphology of the lamellar structure, SEM pictures of the microstructure of the three Ti samples are shown below. These pictures were taken in same location (point 2), therefore we can assume that the cooling rates for these three samples were approximately the same and no other factor affecting the lamellar structure except the Cr content.

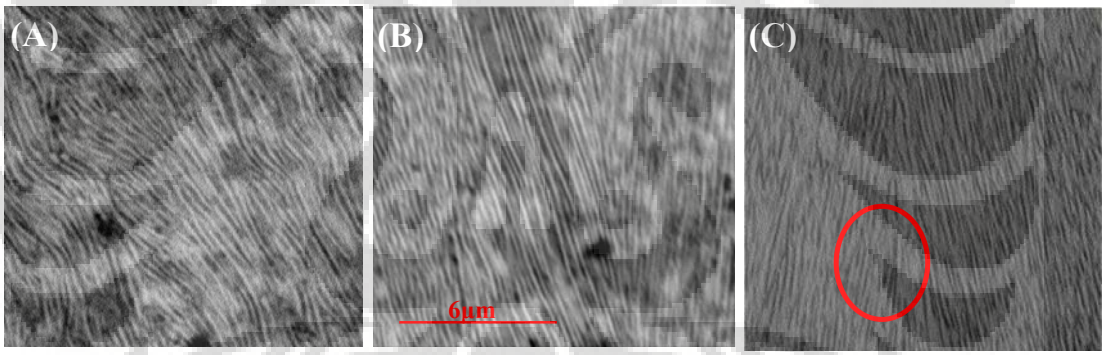

Figure 4.15. Lamellar structure in the three Ti samples (magnification: 15.000x); (a) Ti-Si eutectic, (b) Ti-Si eutectic + 0.02wt% Cr and (c) Ti-Si eutectic + 0.2wt% Cr. These pictures were taken in same location (point 2), therefore the cooling rates were approximately the same.

From the SEM pictures obtained, it is clear that Cr obviously had an effect on the morphology of the lamellar structure. This conclusion is based on the founding that the lamellae in Ti-Si eutectic are a bit wavy (not perfectly straight), and this waviness disappear as ternary addition of Cr is introduced into the alloy. And when the Cr content is increased to 0.2wt%, another change in the morphology of the lamellar structure had occurred, where the lamellae are now become interconnected in some areas (red circle). Furthermore, the lamellar spacing is also found to be affected by the Cr content, since the SEM images show that the lamellar spacing is becomes smaller when Cr (0.02wt%) is added into the alloy. And more addition of Cr up to 0.2wt% leads to a further refinement in lamellar spacing.

IV. 3. Mechanical Properties (Ball Indentation Test)

✓ ***Lamellar Spacing vs Strengthening Factor***

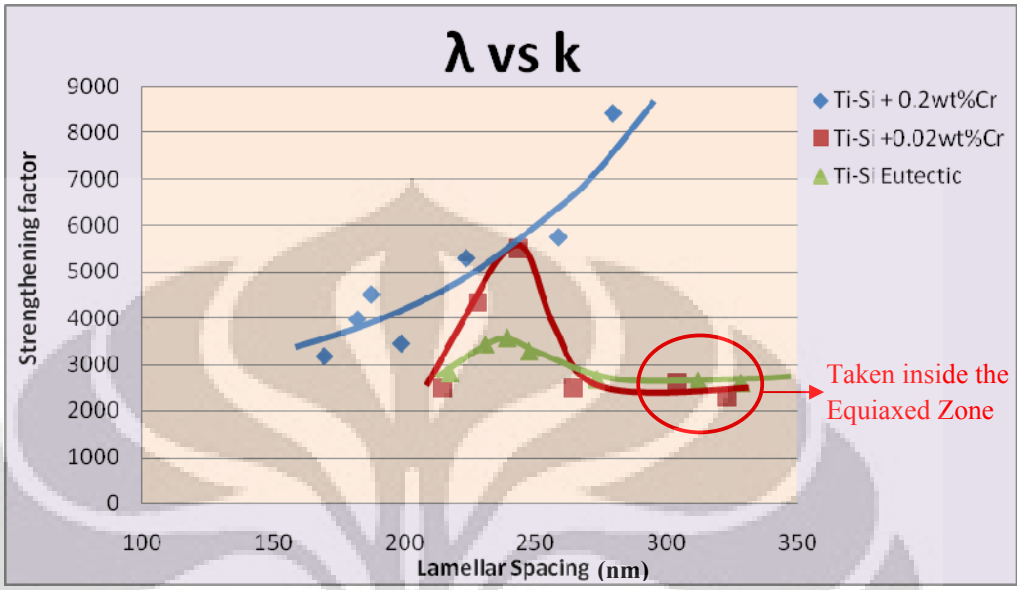

Figure 4.16. Graph showing the relationship between the lamellar spacing and the strengthening factor for the three titanium samples.

✓ ***Lamellar Spacing vs Work Hardening Coefficient***

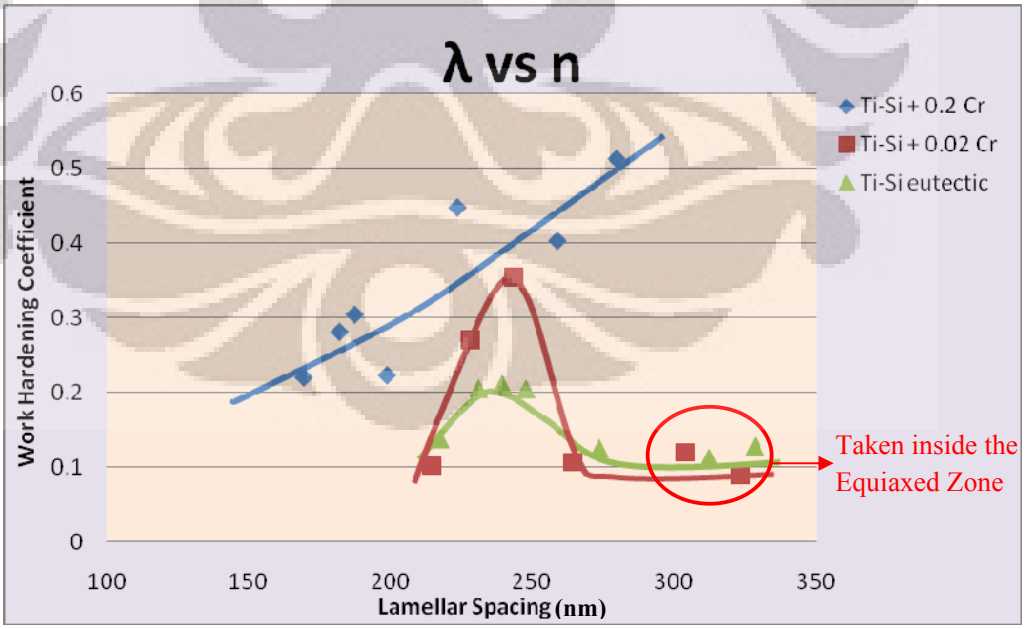

Figure 4.17. Graph showing the relationship between the lamellar spacing and the Work Hardening Coefficient for the three titanium samples.

✓ ***Lamellar Spacing vs Theoritical UTS***

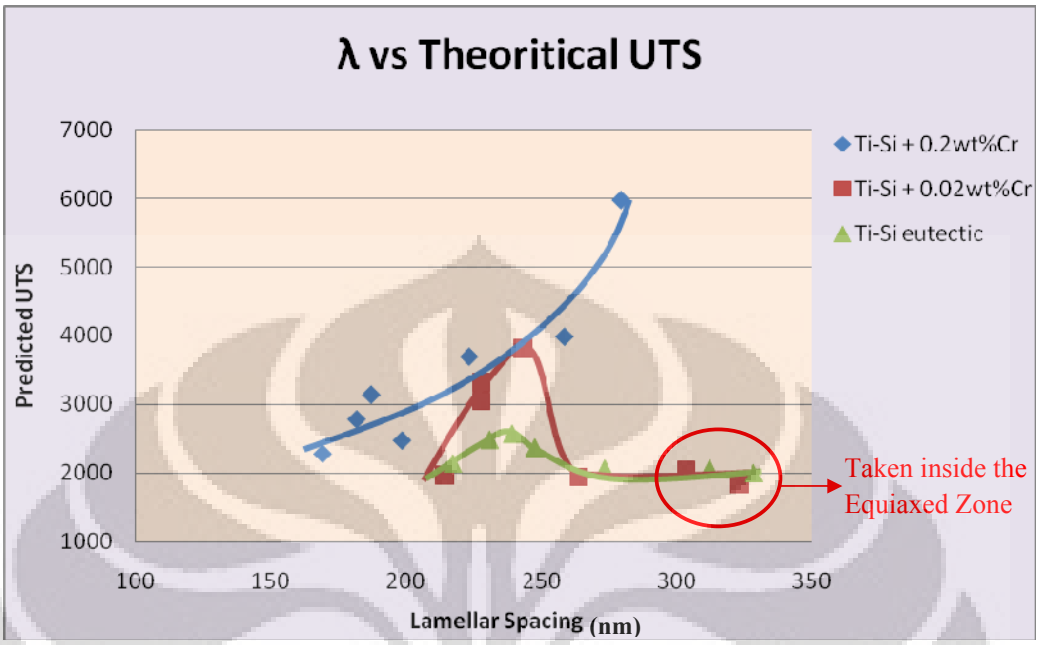

Figure 4.18. Graph showing the relationship between the lamellar spacing and the Predicted UTS for the three titanium samples.

From the graphs obtained, it is clear that the strengthening factor, work hardening coefficient and the predicted UTS are having the same shape of curve when they are plotted against the lamellar spacing. According to the graphs, we can see that the relationship between the strength and the lamellar spacing in both Ti-Si eutectic and Ti-Si eutectic +0.02wt%Cr samples is a HallPetch-like relationship, where the strength of the material increases with a decrease in lamellar spacing. The reason behind this is because in material with smaller lamellar spacing, more lamellar/matrix interfaces exist. These interfaces act as a hindrance for dislocation movement, resulting in a higher value of strength. However, the strength of these two specimens reaches its critical value when the lamellar spacing is about 240 nm. Further from this point, the strength is decreases as the lamellar spacing becomes smaller. The only difference between Ti-Si eutectic and Ti-Si eutectic +0.02wt%Cr samples is that the maximum value of the theoretical UTS achieved at the critical point is higher in Ti-Si eutectic + 0.02wt%Cr sample. Note that there are two points on the right side of the curve that shows an independency of work hardening coefficient on the lamellar spacing. This is because these two measurements were taken inside the equiaxed zone where the lamellar spacing seems to be no longer the factor that dominates the deformation.

As we can see from the graph that the behavior of the work hardening coefficient, strengthening factor and work hardening coefficient in Ti-Si+0.2wt%Cr is different with the other two samples in a way that there is a continual softening as the lamellar spacing becomes smaller. At the moment, the reason for this is still unknown, therefore, further investigation by using TEM is required to observe the deformation mechanism in this particular sample.

CHAPTER IV
CONCLUSION AND FUTURE WORKS

The results of the project can be compiled into some points as the following:

1. The lamellar spacing becomes smaller as the cooling rate is increased.
2. The addition of Cr on Ti-Si eutectic leads to a refinement in the lamellar spacing. Moreover, The morphology of the lamellar structure has found to be affected by the Cr content, where small addition of Cr (0.02wt%) eliminates the waviness of the lamellae occurred in Ti-Si eutectic. And an increase in Cr content to 0.2wt% leads to interconnectivity between the lamellae.
3. There are two different zones present on the microstructure of the three Ti samples, which are columnar and equiaxed zones. The main difference between these two zones is that the lamellae in columnar zones are having their preferential growth direction oriented parallel to the heat extraction, whereas in equiaxed zones, the orientation of the lamellae is different in each grain. In addition, it is also found that the size of the equiaxed zone is become much smaller when the Cr content is increased up to 0.2wt%.
4. From the data obtained, we can conclude that the dependency of theoretical UTS on the lamellar spacing in both Ti-Si eutectic and Ti-Si eutectic +0.02wt%Cr is a HallPetch-like relationship, where the strength is increased when the lamellar spacing is reduced. However, there is a critical point (when the lamellar spacing is approximately 240 nm) where further from this point, the strength of the material is decreases as the lamellar spacing is becomes smaller.
5. The dependency of the theoretical UTS, work hardening coefficient and the strengthening factor on the lamellar spacing in Ti-Si eutectic + 0.2wt%Cr sample is different with the other two samples, in a way that there is a continual decrease as lamellar spacing becomes smaller. And since the reason for this is still unknown, therefore further investigation by using TEM is required to observe the deformation mechanism of this particular sample.

Future Work:

1. Further characterization of the phases present, especially in the Ti-Si eutectic +0.2wt%Cr sample will be performed by using SEM, TEM and XRD. Moreover the crystallographic relationship between the two lamellar phases present will also observed.
2. In addition to this, the deformation mechanism of the three samples will be determined in order to find out the reason behind the difference in dependency of theoretical UTS, strengthening factor and work hardening coefficient on the lamellar spacing in Ti-Si eutectic + 0.2wt%Cr sample.

REFERENCES

1. *http://ezinearticles.com/?Titanium-and-Titanium-Alloys&id=1720441*
2. R. Saha, T. Nandy and R. Misra, *Scripta Metall*. 26 (1991) p. 2637
3. Lütjering, Gerd, Williams, James C. *Titanium (Engineering Materials and Processes) 2nd edition*. (2007) p. 1-15
4. W. Kurz, C. Bezencon, M. Gaumann. *Columnar to Equiaxed Transition in Solidification Processing.* Science and Technology of Advanced Materials 2. (2001) p. 185-191
5. *http://en.wikipedia.org/wiki/Casting_(metalworking)*
6. B. Chalmers: *Principles of Solidification*,Wiley, New York, NY, 1964, p. 255.
7. N. Fatahalla, M. Haviz. M. Abdulkhalek. *Effect of microstructure on the mechanical properties and fracture of commercial hypoeutectic Al-Si alloy modified with Na, Sb and Sr*. J Mat Sci 34 (1999) p. 3555-3564
8. http://www.crct.polymtl.ca/FACT/phase_diagram.php?file=Si-Ti.jpg&dir=SGTE
9. R. Saha, T. Nandy and R. Misra, *Scripta Metall*. 23 (1989) p. 81
10. J.D. Hunt. *Patterns Formation in Solidification*. Science and Technology of Advanced Materials 2 (2001) 147-155
11. *ASTM E112 "test methods for determining the average grain size"*
12. A. E. W. Jarfors. *Solidification behaviour of Al–7% Si–0.3% Mg during rotary spray forming.* J Mat Sci. 33 (1998) p. 3907 – 3918
13. Goutam Das, Sabita Ghosh, and S.K. Sahay. *Mat. Letters*. Vol 59 (2005) p. 2264